Removal of Lead and Cadmium Ions from Aqueous Solution by Polyvinyl alcohol-modified Kaolinite Clay: A Novel Nano-clay Adsorbent

E.I. Unuabonah, B.I. Olu-Owolabi, K.O. Adebowale and L.Z. Yang

Reprinted from

Adsorption Science & Technology

2008 Volume 26 Number 6

Multi-Science Publishing Co. Ltd.
5 Wates Way, Brentwood, Essex CM15 9TB, United Kingdom

Removal of Lead and Cadmium Ions from Aqueous Solution by Polyvinyl alcohol-modified Kaolinite Clay: A Novel Nano-clay Adsorbent

E.I. Unuabonah[1*], B.I. Olu-Owolabi[2], K.O. Adebowale[2] and L.Z. Yang[3] *(1) Department of Pure and Industrial Chemistry, College of Sciences, Federal University of Petroleum Resources, PMB 1221, Effurun, Nigeria. (2) Department of Chemistry, Faculty of Science, University of Ibadan, Nigeria. (3) Institute of Soil Science, Nanjing, Jiangsu Province, P. R. China.*

(Received 15 May 2008; revised form accepted 16 October 2008)

ABSTRACT: Kaolinite clay was modified with polyvinyl alcohol (PVA) to obtain a PVA–nano-clay adsorbent. X-Ray diffraction measurements of the adsorbent showed no observable change in the d-spacing of its crystal lattice. Scanning electron microscopy of the PVA-modified nano-clay adsorbent indicated the presence of irregular crystal structures. Infrared spectroscopy suggested that the PVA–nano-clay adsorbent basically possessed outer –OH functional groups. This adsorbent was found to have an adsorption capacity of 56.18 mg/g for Pb^{2+} ions and 41.67 mg/g for Cd^{2+} ions. The adsorption data obtained was well explained by the Diffuse Layer Model (DLM), which implies that the adsorption of both metal ions onto the modified adsorbent was via an inner-sphere surface complexation mechanism. The ΔH^0 values for the adsorption of both metal ions onto the PVA–nano-clay were –12.48 kJ/mol for Pb^{2+} ions and –13.49 kJ/mol for Cd^{2+} ions, with both ions exhibiting negative adsorption entropies. Data-fitting indicated that both the PVA–nano-clay and the unmodified adsorbent possessed homogeneous and heterogeneous adsorption sites. Virtually complete desorption (ca. 99%) of both metal ions occurred from PVA–nano-clay within 3 min.

1. INTRODUCTION

The sorption of metal ions by mineral substrates is very important for wastewater treatment and soil chemistry (Ikhsan *et al*. 1999). Several methods have been adopted over the years for the removal of metal ions dissolved in water and industrial wastewaters; these include chemical precipitation, conventional coagulation, reverse osmosis, ion-exchange and adsorption. However, various factors control the choice of adsorbent for a wastewater treatment method, including the concentration of metal ions in the wastewater, the efficiency/cost ratio and the adsorption capacity of the adsorbent.

Adsorption is one of the most popular and efficient processes for the removal of heavy metal ions from industrial wastewater. Since the volume of water to be purified is generally large, the adsorbent to be used in the process should possess a high selectivity with respect to the heavy metal ion(s) concerned, be non-toxic, capable of regeneration, easily recoverable from filters, relatively cheap and readily available (Gupta and Bhattacharyya 2006). The use of adsorbents has also been found to circumvent the production of large amounts of sludge usually associated with some other alternative wastewater-treatment techniques like precipitation (Ho and McKay 1999).

*Author to whom all correspondence should be addressed. Current address: Department of Chemical Sciences, College of Natural Sciences, Redeemer's University, Mowe, Ogun State, Nigeria. E-mail: iyaemma@yahoo.com.

Several methods have been employed to improve the cation-exchange capacity (CEC) of clay minerals. Some of these include activation (Suraj *et al*. 1998), pillaring or intercalation (Frost *et al*. 1997, 1999, 2002), and chemical modification of the surface using inorganic complex-forming ions (Sidheswara *et al*. 1990) or organic-based complex-forming ions (Dais Filho *et al*. 1995). Recently, Manohar *et al*. (2002) and Dais Filho *et al*. 1995) have reported that 2-mercaptobenzothiazole-impregnated clay surfaces can be used for the removal of some heavy metal ions from water samples. In recent years, there has been a pronounced tendency to utilize mechanically stable synthetic or natural solid matrices in many applications, such as chemically-bonded silica in chromatography (Sang-Mo and Dixon 2002; Jal *et al*. 2004). These and other previous research works suggest that chemically-modified clay minerals present a new and promising class of adsorbent materials for water purification and industrial wastewater treatment. The use of clay minerals for the adsorption of metal ions from aqueous solutions has been widely studied. It has been found that these clay minerals would have as great an efficiency as activated carbon if the difficulty experienced in the recovery of the adsorbent from filters after use could be overcome. This also makes the regeneration and possible re-use of a clay adsorbent very difficult.

To address the problem of the recovery of adsorbent/resin from filters after use, a novel water-stable ion-exchange resin for the adsorption of metal ions has been produced from locally obtained kaolinite clay using polyvinyl alcohol (PVA) as the modifying reagent. Variables such as pH, adsorbate concentration, ionic strength, time, temperature and adsorbent weight that could affect the adsorption of Pb^{2+} or Cd^{2+} ions onto the PVA-modified clay adsorbent were considered. The thermodynamics of the adsorption of these metal ions onto both PVA-modified kaolinite clay and unmodified kaolinite clay adsorbents have been studied with a view to providing data that would be helpful in the design of an efficient but cost-effective adsorption system from PVA-modified kaolinite clay adsorbent.

2. MATERIALS AND METHODS

Kaolinite clay was obtained from Ubulu-Ukwu, Delta State, Nigeria with stones and other heavy particles being removed from the sample after collection. A portion of the raw kaolinite in a 1 ℓ beaker was maintained in suspension in doubly de-ionized water for several hours. This material was further purified using the method of Moore and Reynolds (1989).

2.1. Modification of the clay sample

The kaolinite clay was treated with 2 M HNO_3 for 1 h to effect its oxidation. The resulting material was centrifuged, washed several times with de-ionized distilled water and then dried in an oven at 343 K.

A known weight (50 g) of the kaolinite clay sample was then taken, 100 mℓ of de-ionized distilled water added to it and the resulting suspension heated to boiling and treated with a 10% PVA/formaldehyde solution. The resulting mixture was rapidly agitated until the kaolinite resin gel formed, when the temperature of the suspension was maintained at 343 K. After formation of the kaolinite resin gel, the temperature of the system was increased to 353 K and 5% PVA added to generate a coating. At this stage, the system was maintained at 353 K for 1 h. This procedure was repeated three times before the sample was washed thoroughly with de-ionized distilled water and dried in an oven at 333 K.

Once dried, the very hard kaolinite clay–resin (PVA–nano-clay adsorbent) was broken into particles and sieved to the desired particle size (+220 μm). X-Ray diffraction (XRD) spectra of both

the unmodified and PVA–nano-clay adsorbents were obtained using a Philips analytical X-ray spectrometer (PW 1710) employing Cu Kα radiation at 40 kV and 40 mA. The XRD patterns were recorded over the 2θ range from 1.5º to 50º at a scanning speed of 0.02º at 2θ/s. Scanning electron microscopy (SEM) for both adsorbents was undertaken using a Philips EDAX microscope. The infrared spectrum of the polyvinyl-modified kaolinite clay adsorbent sample was obtained via a PerkinElmer IR spectrometer employing KBr wafers. IR studies of the unmodified kaolinite clay adsorbent have been reported previously (Unuabonah *et al*. 2007). The point of zero charge (PZC) of both adsorbents was obtained employing the method of Kinniburgh *et al*. (1976), while their specific surface areas (SSAs) were determined using the method of Sears (1956). Similarly, the cation-exchange capacity (CEC) of the PVA–nano-clay sample was determined using the ammonium acetate method of Chapman (1965). The CEC of the unmodified kaolinite clay sample has been determined previously by Adebowale *et al*. (2006) employing the same method.

2.2. Adsorption studies

2.2.1. Effect of adsorbent dose

Stock solutions of $Pb(NO_3)_2$ and $Cd(NO_3)_2$ at a concentration of 1 g/ℓ were prepared in standard 1 ℓ flasks. These stock solutions were then employed to obtain suitable working concentrations of the metal ions under study. Known volumes (20 mℓ) of each of the Pb^{2+} and Cd^{2+} ion solutions (at 300 mg/ℓ concentration) were then placed in polyethylene bottles of 120 mℓ volume into which 0.1–1.0 g of the PVA–nano-clay sample was introduced. The samples were agitated for 5 h to achieve equilibrium, preliminary experiments having shown that adsorption equilibrium was established in 4.5 h for both metal ions. The pH value of the metal ion solutions was maintained at 5.5 ± 0.05 in all cases. After agitation, the suspensions were centrifuged at 1500 rpm for 15 min and the supernatant stored for Pb^{2+} or Cd^{2+} ion analysis.

2.2.2. Effect of pH value

To study the effect of pH on the behaviour of the individual samples, 20 mℓ volumes of each of the metal ion solutions at 300 mg/ℓ concentration were added individually to 0.1 g of both the unmodified and PVA–nano-clay samples contained in polyethylene bottles of 120 mℓ volume. The pH values of the suspensions thus obtained were adjusted within the range 4.0 ± 0.05 to 7.0 ± 0.05 by the addition of either 0.1 M NaOH or 0.1 M HCl. The resulting systems were agitated for 5 h, following which the suspensions were centrifuged at 1500 rpm for 15 min and the supernatant stored for Pb^{2+} or Cd^{2+} ion analysis.

2.2.3. Adsorption equilibrium studies

For equilibrium studies, the pH value of each of the metal ion solutions in contact with the polyvinyl alcohol-modified adsorbent (PVA–nano-clay sample) was adjusted to a value of 5.5 ± 0.05. Batch adsorption experiments were performed at room temperature (301 ± 1 K) using capped polyethylene bottles of 120 mℓ volume containing 20 mℓ of the metal ion solutions at 60–400 mg/ℓ concentration and 0.1 g of the modified PVA–nano-clay adsorbent. Such systems were shaken on a rotary shaker at 100 rpm for 5 h and then centrifuged at 1500 rpm for 15 min with the supernatant being stored for Pb^{2+} and Cd^{2+} ion analysis.

Data obtained previously by Adebowale *et al*. (2006) for the unmodified kaolinite clay sample showed that an increase in the pH value of the system encourages metal ion precipitation in the

form of hydroxides, with this in turn enhancing metal ion adsorption. It is therefore possible that precipitation could also account for some of the metal ion adsorbed. To ascertain the approximate amounts of metal ions precipitated, samples of the various systems containing the same concentration of metal ions as those employed for the adsorption studies and at the same pH values were allowed to stand for a period of 6 h, with the concentration of metal ions in the supernatant being subsequently determined. The results obtained indicated that only a small fraction (< 5%) of the metal ions were precipitated from their respective solutions over the pH ranges employed for the adsorption studies in the present work.

2.3. Thermodynamic studies

The thermodynamics of the adsorption of Pb^{2+} or Cd^{2+} ions onto the PVA–nano-clay adsorbent were studied by adding 0.1 g of the adsorbent to 20 mℓ volume samples of the individual metal ion solutions at various concentrations (60–400 mg/ℓ) at a pH value of 5.5 ± 0.05. These systems were then agitated, with samples being collected after 5 h for metal ion analysis. The above procedure was carried out at 298 K, 313 K and 323 K, respectively, thereby allowing the thermodynamic parameters, ΔH^0, ΔS^0 and ΔG^0, for the adsorption process to be calculated using the relationship:

$$\ln b = \Delta S/R - \Delta H/RT \quad (1)$$

where b is the Langmuir constant related to energy. The linear plot of ln b versus 1/T yields a slope and intercept whose values correspond to ΔH^0 and ΔS^0, respectively. These values can then be used to compute ΔG^0 by applying the Gibbs relationship:

$$\Delta G^0 = \Delta H^0 - T\Delta S^0 \quad (2)$$

In deriving the values of the thermodynamic parameters, it is assumed that the enthalpy does not change with temperature.

2.4. Effect of electrolyte ionic strength

The effects of both the nature of the electrolyte and its ionic strength were studied using $NaNO_3$, NaCl, $CaCl_2$ and $Ca(NO_3)_2$ at three different concentrations (0.1, 0.01 and 0.001 M). Thus, the various weights of electrolyte necessary for the preparation of each concentration were added to the weights of Pb^{2+} or Cd^{2+} ion salts required to prepare the various concentrations of the metal ions, mixed and made up to the standard mark using distilled, de-ionized water. Subsequently, 20 mℓ volumes of these solutions were added to 0.1 g of the PVA–nano-clay adsorbent. The pH values of the resulting suspensions were adjusted to the same values as used for the equilibrium studies, and the various systems agitated for 5 h. These were subsequently centrifuged at 1500 rpm for 15 min, the supernatants collected and their Pb^{2+} or Cd^{2+} ion contents determined. Previous studies by Adebowale *et al*. (2006) have provided data for the effects of electrolytes on suspensions of the unmodified kaolinite clay.

2.5. Desorption studies

For such studies, 20 mℓ of 0.1 M HCl was added to 0.1 g of the PVA–nano-clay sample which had been initially saturated with 60 mg/ℓ solutions of Pb^{2+} or Cd^{2+} ions and then thoroughly washed to remove any excess of such ions. This mixture was agitated for 30 min, following which

the supernatants were collected for Pb^{2+} or Cd^{2+} ion analysis. The amount of metal ions desorbed was obtained from the difference between the amount of metal ions fully loaded onto the adsorbent and the amount of the same in solution. The regenerated adsorbents were re-used in the adsorption of 60 mg/ℓ solutions of Pb^{2+} or Cd^{2+} ions from aqueous solution to ascertain their adsorption efficiencies for both metal ions after regeneration.

All the collected samples were analyzed for their Pb^{2+} or Cd^{2+} ion content using an ICPAES (Inductively Coupled Plasma Atomic Emission Spectroscopy) IRIS Advantage instrument (Thermo Fisher, Epsom, Surrey, U.K.). The amounts of Pb^{2+} or Cd^{2+} ions adsorbed were calculated from the relationship:

$$q_e = \frac{(C_0 - C_e)V}{1000W} \tag{3}$$

where C_0 is the initial concentration of metal ions (mg/ℓ), C_e the equilibrium concentration of metal ions (mg/ℓ), V is the volume of metal ion solution employed (mℓ), W is the weight of adsorbent used (g) while q_e is the amount of metal ions adsorbed (mg/g).

2.6. Theoretical equilibrium adsorption models

2.6.1. The Langmuir isotherm

The Langmuir equation may be written as:

$$q_e = Q^0 bC_e/(1 + bC_e) \qquad (\text{non-linear form}) \tag{4}$$

$$C_e/q_e = 1/Q^0 b + C_e/Q^0 \qquad (\text{linear form}) \tag{5}$$

where q_e is the amount of solute adsorbed at equilibrium per unit weight of adsorbent (mg/g), C_e is the equilibrium concentration of solute in the bulk solution (mg/ℓ), Q^0 is the monolayer adsorption capacity (mg/g) and b is a constant related to the energy of adsorption (ℓ/g). The latter is the reciprocal value of the concentration at which half-saturation of the adsorbent has been attained.

2.6.2. The Freundlich isotherm

The Freundlich equation may be written as:

$$q_e = K_F C_e^{1/n} \qquad \text{(non-linear form)} \tag{6}$$

$$\log q_e = \log K_F + \tfrac{1}{n} \log C_e \qquad (\text{linear form}) \tag{7}$$

where q_e is the amount of solute adsorbed at equilibrium per unit weight of adsorbent (mg/g), C_e is the equilibrium concentration of solute in the bulk solution (mg/ℓ), K_F is a constant indicative of the relative adsorption capacity of the adsorbent (mg/g) and 1/n is a constant indicative of the intensity of the adsorption process.

2.6.3. The Toth isotherm

This is an isotherm which is based on the Langmuir isotherm. It assumes both a left-hand widened Gaussian energy distribution and a continuous distribution of site affinities (Orhan *et al*. 1998). The corresponding equation may be written as:

$$q_e = KC_eQ^0/\left\{1 + \left(KC_e\right)^n\right\}^{1/n} \tag{8}$$

where the quantities q_e, K, C_e, Q^0 and n are same as those included in the Freundlich isotherm equation.

2.6.4. The Langmuir–Freundlich isotherm

This is a combination of the Langmuir and Freundlich isotherms which is assumed to provide a better description of adsorption onto a heterogeneous surface. The equation can be written as:

$$q_e = \left(KC_e\right)^n Q^0/\left\{1 + \left(KC_e\right)^n\right\} \tag{9}$$

where the quantities q_e, K, C_e, Q^0 and n are same as those included in the Freundlich isotherm equation (Orhan *et al*. 1998).

2.6.5. The Henderson isotherm

The Henderson isotherm equation (Basar 2006) is suitable for multilayer adsorption involving hetero-porous solids. The equation can be written as:

$$\ln\left[-\ln\left(1 - C_e\right)\right] = \ln K + n\ln q_e \qquad \left(\text{linear form}\right)_e \tag{10}$$

$$q_e = \left[1/\left(K\ln C_e\right)\right]^{1/n} \qquad \left(\text{non-linear form}\right) \tag{11}$$

where n and K are constants, and q_e and C_e are same as employed in the Langmuir isotherm.

3. RESULTS AND DISCUSSION

3.1. Physicochemical characteristics

The specific surface area (SSA) of the PVA–nano-clay was 7.92 m^2/g while the SSA of unmodified kaolinite clay adsorbent was 10.56 m^2/g. This decrease in the value of the SSA did not influence the efficiency of the PVA–nano-clay adsorbent in any way, as it was more efficient than the unmodified adsorbent in the adsorption of Pb^{2+} and Cd^{2+} ions. This was because the decrease in specific surface area was well compensated for by the increase in the number of active sites on the surface of the modified adsorbent available for the adsorption of metal ions.

The points of zero charge of the unmodified and PVA–nano-clay adsorbents were found to be 4.40 and 4.25, respectively. The CEC of the PVA–nano-clay adsorbent was determined as

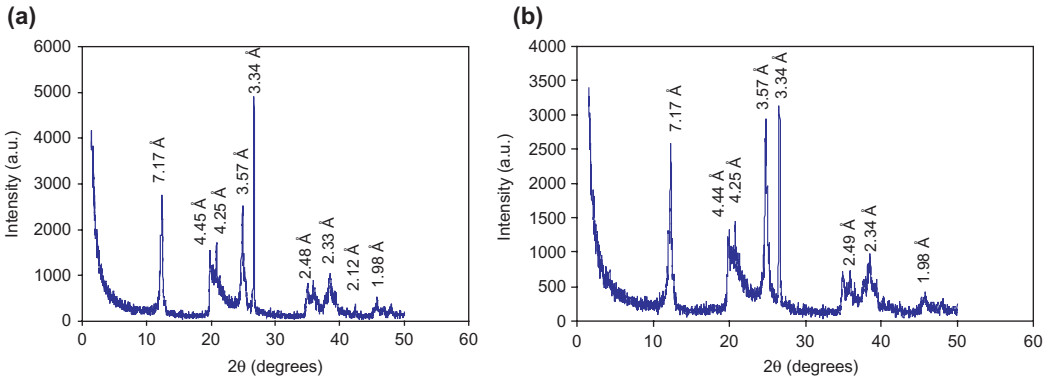

Figure 1. X-Ray diffraction spectrum of (a) the unmodified kaolinite clay adsorbent and (b) the PVA–nano-clay adsorbent.

51.04 mequiv/100 g adsorbent while the CEC of the unmodified kaolinite clay as determined previously (Adebowale *et al*. 2006) was 7.81 mequiv/100 g clay.

Figure 1(a) shows the X-ray diffraction spectrum of the unmodified adsorbent which exhibits peaks at 7.17 Å (001), 4.25 Å, 3.57 Å (002), 3.34 Å, 2.56 Å, 2.49 Å, 2.33 Å, 2.12 Å and 1.98 Å, respectively, corresponding to kaolinite, quartz, kaolinite, illite + quartz, goethite, goethite, gibbsite, gibbsite and dickite, respectively (Moore and Reynolds 1989). The prominent peaks found in this X-ray diffraction spectrum suggest that the original clay employed was a mixed kaolinite/illite mineral (Gupta *et al*. 2004). These same peaks also occur in the X-ray diffraction spectrum of the PVA–nano-clay adsorbent with no significant shift in the d-spacing, although the intensity of the quartz/illite peak was somewhat diminished [Figure 1(b)].

Figures 2(a) and (b) show the SEM micrographs for the unmodified and PVA–nano-clay adsorbents. It will be seen from Figure 2(a) that the unmodified adsorbent consisted of irregular

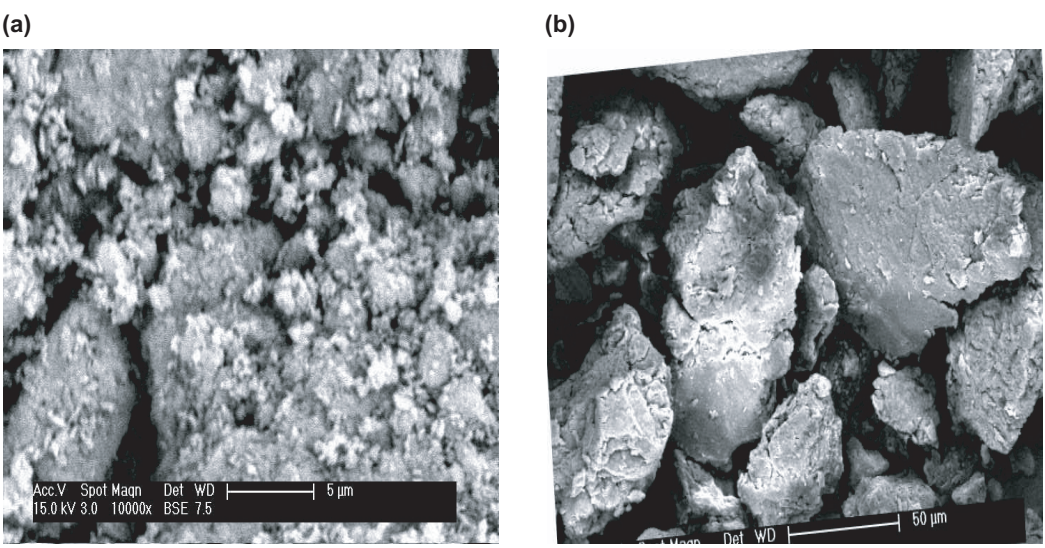

Figure 2. Scanning electron micrograph of (a) the unmodified kaolinite clay and (b) the PVA–nano-clay adsorbent.

shaped particles where some white particles appeared on the surfaces of the mineral particles. These white particles are likely to be non-clay minerals containing sodium, potassium, calcium, iron and magnesium (Galan *et al*. 1996). In contrast, the particles of the PVA–nano-clay adsorbent were clumped together [see Figure 2(b)] with no definite structure.

3.2. IR spectral analysis

The band assignments arising from the IR spectra of both the unmodified and PVA–nano-clay adsorbents [Figures 3(a) and (b), respectively] are listed in Table 1. The IR band assignments for the unmodified kaolinite clay sample were fully described in our previous paper (Unuabonah *et al*. 2007) but have been reproduced here for comparative purposes. The absorption band at 3668.3 cm^{-1} for the unmodified sample corresponds to the inner surface –OH stretching vibration while those at 1034.4 cm^{-1} and 918.7 cm^{-1} correspond to the Si–O and Al–OH bending vibrations, respectively.

An absorption band at 3696.74 cm^{-1} in the spectrum of the PVA–nano-clay adsorbent indicated the presence of inner surface –OH groups, while a corresponding broad and prominent band at 3440.96 cm^{-1} indicated the existence of outer –OH groups. This latter band was not present in the spectrum of the unmodified adsorbent (see data in Table 1). The outer –OH groups are possibly the main adsorption sites in the PVA–nano-clay adsorbent. Bands corresponding to Si–O and Al–O groups, which occurred at 1034.4 cm^{-1} and 918.7 cm^{-1}, respectively, in the spectrum of the unmodified kaolinite sample, were displaced to 1006 cm^{-1} and 912.62 cm^{-1}, respectively, in the spectrum of the PVA–nano-clay adsorbent. These latter peaks were also broader and more prominent than the corresponding peaks in the spectrum of the unmodified kaolinite clay adsorbent. The band at 3668.3 cm^{-1} for the inner –OH groups of the unmodified kaolinite clay adsorbent was shifted to 3696.74 cm^{-1} for the PVA–nano-clay adsorbent. This indicates that modification may have also occurred at these sites in the latter adsorbent.

3.3. Effect of adsorbent dosage

The variation in the amount of Pb^{2+} or Cd^{2+} ions adsorbed from a 300 mg/ℓ solution of the metal ions onto various dosages of the PVA–nano-clay adsorbent was studied to ascertain the effect of such dosages on the ion uptake from aqueous solution. Plots of the corresponding sorption curves are depicted in Figure 4.

Increasing the dosage of the PVA–nano-clay adsorbent over the range 0.1–1.0 g resulted in a decrease in the equilibrium adsorption capacity, q_e, of the adsorbent (Figure 4). A similar trend has been reported by Ho and Ofomaja (2005) in the adsorption of Pb^{2+} ions by palm kernel fibre and by Gupta and Bhattacharyya (2006) in the adsorption of Ni(II) ions onto kaolinite. The decrease in the equilibrium adsorption capacity, q_e, of adsorbents towards metal ions with increasing dosages of adsorbent can be attributed to a decrease in the surface area of the adsorbent with increasing particle aggregation and a reduction in the number of adsorption sites as a direct result of such particle aggregation (Shukla *et al*. 2002; Bordas and Bourg 2001).

The relationship between the adsorbent dosage and the equilibrium adsorption capacity, q_e, may be found by linear extrapolation in conjunction with the correlation coefficient (r^2). The corresponding relationship may be expressed as:

$$q_e = Sm_s + Y \tag{12}$$

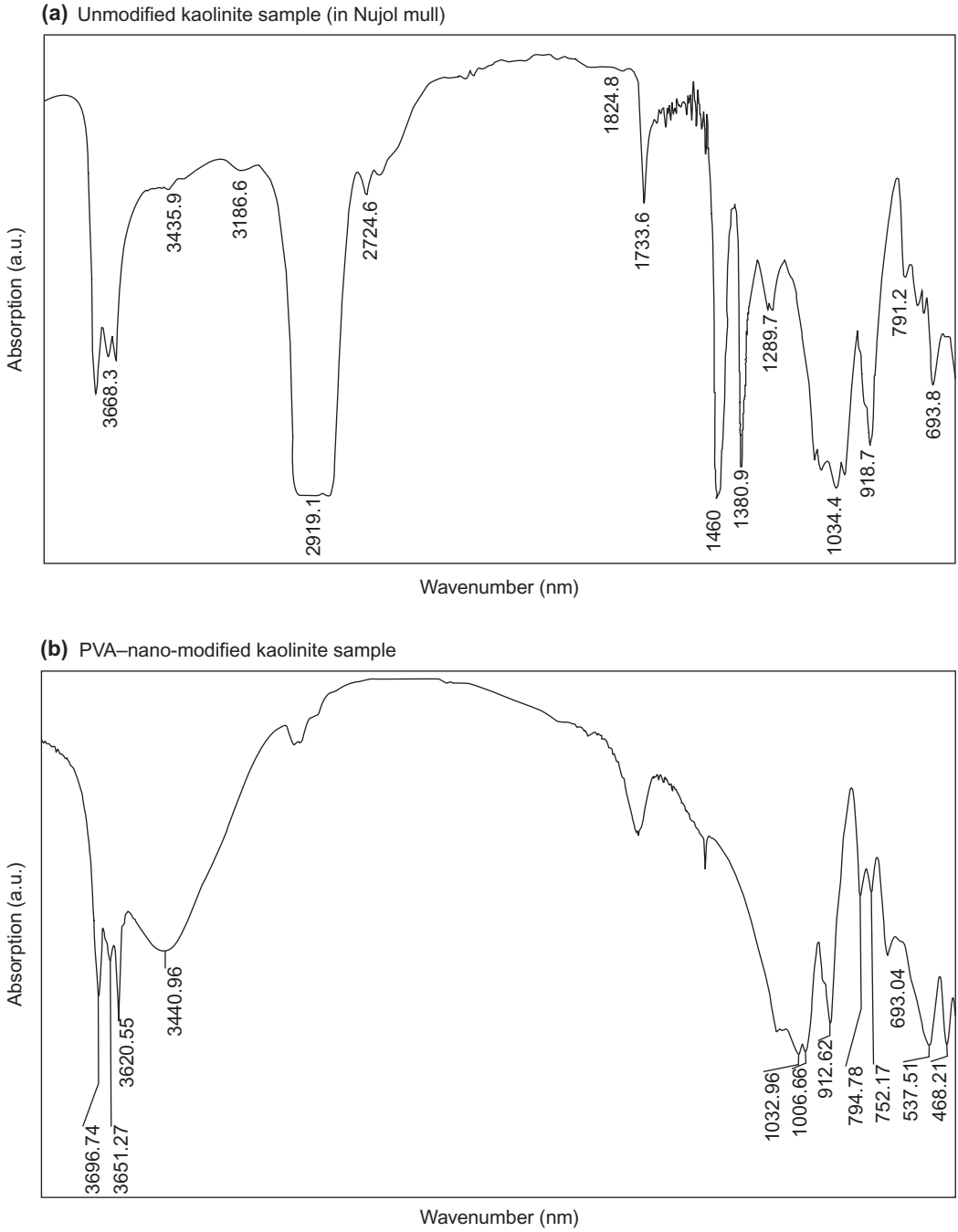

Figure 3. IR spectrum of (a) the unmodified kaolinite clay [reproduced from Unuabonah *et al*. (2007)] and (b) the PVA–nano-clay adsorbent.

TABLE 1. Band Assignments from IR Spectra of Unmodified and PVA-modified Kaolinite Clays

IR frequencies		Band assignments
Unmodified[a]	PVA–nano-clay	
3668.3	3696.74, 3651.27	Inner surface –OH stretching vibration
–	3440.96	Outer surface –OH stretching vibration
2919	–	$-CH_3$ (Nujol mull)
1733.6	–	–OH bending vibration
1034.4	1032.96, 1106.66	Si–O, Si–O–MR[b] bending vibration
918.7	912.62	Al–O, Al–O–MR bending vibration
792	794.98, 752.17	Si–O stretching vibration
693.8	693.04	Si–O stretching vibration
–	537.51	Al–O–Si deformation

[a]Values reproduced from Unuabonah *et al*. (2007). [b]MR = modifying reagent.

where the constant Y is the maximum adsorption capacity of the adsorbent. When the adsorbent dosage, m_s, approaches zero, the quantity S is related to the adsorption potential of the adsorbent. Negative values of S show that the equilibrium adsorption capacity, q_e, decreases with increasing adsorbent dosage. Equation (12) can be used to predict the amounts of metal ions that will be

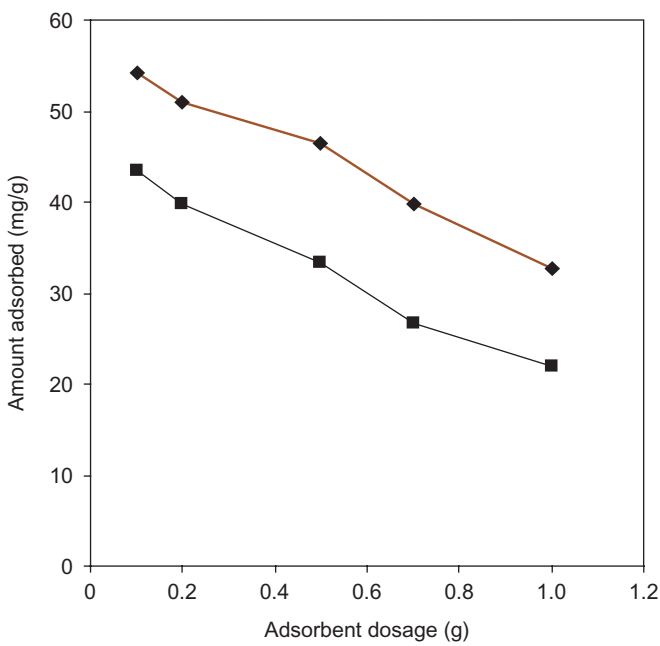

Figure 4. Effect of the dosage of PVA–nano-clay adsorbent on its adsorptive capacity towards (◆) Pb^{2+} or (■) Cd^{2+} ions.

TABLE 2. Values of the Constants Obtained for the Adsorption of Pb^{2+} or Cd^{2+} Ions from the Relationship between the Adsorbent Dose and the Equilibrium Adsorption Capacity

Kaolinite clay sample	Y (mg/g)	S [$(dm^3\ mg)/g^2$]	R^2
PVA–nano-clay (+ Pb^{2+} ions)	86.90	–86.03	0.8394
PVA–nano-clay (+ Cd^{2+} ions)	70.27	–68.20	0.8507

adsorbed by particular weights of either of the adsorbents used in this study. The values of Y and S listed in Table 2 suggest that the PVA–nano-clay adsorbent had a better selectivity towards Pb^{2+} ions than Cd^{2+} ions.

3.4. Effect of pH value

The pH values of the 300 mg/ℓ solutions of Pb^{2+} or Cd^{2+} ions employed were varied over the range 4.0–7.0. The influence of such a variation in pH value on the adsorption of Pb^{2+} or Cd^{2+} ions by the PVA–nano-clay adsorbent is shown in Figure 5.

It will be seen from the figure that the adsorption of both metal ions by the modified adsorbent increased as the pH values of the metal ion solutions increased. Such an enhanced metal ion uptake has also been reported by Orunwense (1996) and by Coston *et al*. (1995) for the adsorption

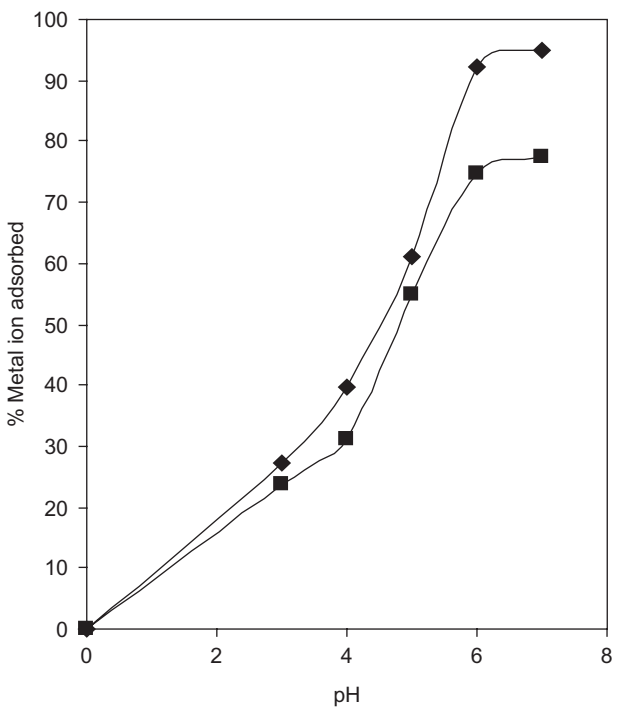

Figure 5. The influence of pH on the adsorption of (◆) Pb^{2+} or (■) Cd^{2+} ions onto the PVA–nano-clay adsorbent.

of Pb^{2+} ions and by Sparks *et al*. (1995) for the adsorption of Cu^{2+}, Zn^{2+}, Co^{2+} and Cd^{2+} ions. This may result from an increase in the overall negative charge on both the unmodified and modified adsorbent samples, especially between pH values of 4.0 and 7.0.

The variation in the extent of adsorption of a divalent cation with pH value at a constant weight of adsorbent and initial metal ion concentration has been expressed by Sposito (1989) as:

$$\ln D = a + b(pH) \tag{13}$$

where $D = f_{adsorb}/f_{soln}$, a and b are empirical constants, while D is the distribution ratio defined as the ratio of the fraction of metal ions adsorbed to the fraction of metal ions in solution. A plot of ln D versus pH is called a Kurbatov plot. The pH value at which D = 1, i.e. when 50% of the added metal ion has been adsorbed and 50% is still in solution, is designated as pH_{50}. The value of pH_{50} is a relative measure of the selectivity of an adsorbent for a series of divalent metal cations (Sposito 1989). The smaller the pH_{50} value, the greater the selectivity of the adsorbent towards the metal cation.

From plots of ln D versus pH (not shown) and the use of equation (13), it was found that the adsorption capacity of the PVA–nano-clay adsorbent towards Pb^{2+} ions was greater than towards Cd^{2+} ions. Thus, at pH_{50} (the pH at which 50% of the metal ion is adsorbed), the value for the Pb^{2+} ion was ca. 4.65 while that for the Cd^{2+} ion was 4.81.

3.5. Adsorption mechanism

It is believed that one of the modes of adsorption of the metal ions under consideration onto the surface of the adsorbent is:

$$M^{2+} + 2(=SOH) \rightleftharpoons =(SO)_2M + 2H^+ \tag{14}$$

where S designates the adsorbent surface. Such an equation is justified by the observed drop in pH value of the equilibrium metal ion solutions from an initial value of 5.5 to between 1.0 and 1.92 for both adsorbents during the adsorption process (Singh *et al*. 2001). Thus, it was observed that as the initial concentration of the metal ion solution was increased, the equilibrium pH of the metal ion in solution decreased from 5.5 to 3.98 for Pb^{2+} ions and from 5.5 to 4.12 for Cd^{2+} ions, respectively, in the presence of the PVA–nano-clay adsorbent. The above relationship was further confirmed by IR data which suggested that the main functional group present on the PVA–nano-clay adsorbent was the –OH group.

It is possible that the active sites present on the PVA–nano-clay are weakly acidic in nature. Thus, with increasing pH, they are gradually deprotonated, thereby making more and more sites available for metal ion uptake. Under acidic conditions, the adsorbent surface acquires a net positive charge as follows:

$$SO^- + H{-}OH \xrightarrow{H^+} S{-}OH_2^+ + OH^- \tag{15}$$

The resulting surface will exhibit a reduced adsorption capacity towards metal ions at low pH values. However, as the pH value increases towards the alkaline region, the adsorbent surface becomes negatively charged thereby favouring the uptake of the metal ions:

$$SOH + OH^- \rightleftharpoons SO^- + H_2O \tag{16}$$

$$SO^- + M^{2+} \rightleftharpoons S{-}O\cdots M^+ \quad (17)$$

$$SO^- + MNO_3^+ \rightleftharpoons S{-}O\cdots MNO_3 \quad (18)$$

Visual MINTEQA2 version 4.0, a chemical speciation software, was used to further clarify the above proposed mechanism for the adsorption of Pb^{2+} or Cd^{2+} ions onto the PVA–nano-clay adsorbent. The Diffuse Layer Model (DLM) was chosen because the number of parameters required for this model is less than that for the Triple Layer Model (TLM) (Langmuir 1997), the formulation of the stoichiometry of the equilibrium problem for the DLM is much simpler than for the Triple Layer Model (Goldberg 1995), and it leads to better results than the Constant Capacitance Model (CCM) (Hohl and Stumm 1976). In our modelling approach, we used a high electrolyte concentration (0.097 M $NaNO_3$) so that ion-exchange adsorption onto the PVA–nano-clay surface sites would be minimized. The concentration of electrolyte employed was such that it could be assumed that the exchange sites on the adsorbent would be well saturated with Na^+ ions, resulting in inner-sphere surface complexation in accordance with the basic assumptions of the DLM. Visual MINTEQA2 version 4.0 input values for the DLM are listed in Table 3.

Using these inputted values for a Pb^{2+} or Cd^{2+} ion solution with an initial metal ion concentration of 100 mg/ℓ, it was observed that the concentration of $=SO^-$ surface adsorption sites assumed on the PVA–nano-clay adsorbent increased as the pH value of the system increased from 4.0 to ca. 9.0 while the concentration of $=SOH_2^+$ surface sites remained virtually zero throughout the pH range studied (see Figure 6). The same trend was observed at higher initial concentrations for both metal ions. This strengthens our earlier proposal that as the pH value increases the surface sites on the PVA–nano-clay adsorbent are gradually deprotonated, thereby making more and more surface sites available for the uptake of metal ions. This is further corroborated by the linear relationship existing between the pH value of the metal ion solution and both the charge density and the surface potential of the adsorbent (Figure 7). However, as the initial concentration of metal ions increased, it was found that the surface potential of the PVA–nano-clay adsorbent decreased slightly, together with a small increase in the charge density of the adsorbent (see Figures 8 and 9). This inverse relationship between the surface potential, charge density and increasing initial concentration of the metal ion is probably due to the small increment in the amount of MNO_3^+ adsorbed (this being the minor ionic species adsorbed by the PVA–nano-clay adsorbent — see Figure 10) with a corresponding decrease in the amount of M^{2+} adsorbed, thereby allowing the

TABLE 3. Diffuse Layer Model Constants Used in this Study as Obtained from Visual MINTEQ 2.30

Selection adsorption model	2-pK DLM
Solid concentration (g/ℓ)	10
Specific surface area (m^2/g)	7.98
Site concentration (low affinity)	0.01 mM
(high affinity)	60 mM
Site density (sites/nm^2)	452.933
Geometry of adsorbent	planar
Temperature	298 K

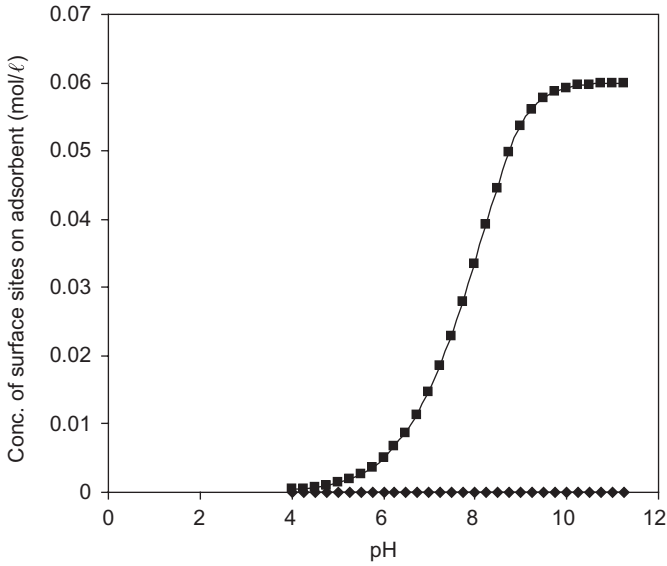

Figure 6. Relationship between the surface sites on the PVA–nano-clay adsorbent (◆, $=SOH_2^+$; ■, $=SO^-$) and the pH value of the system. Data obtained from model results using Visual MINTEQA2 version 4.0 software.

adsorbent surface to acquire a small amount of positive charge with a consequent positive impact on the overall charge density of the adsorbent.

However, this positive impact of increasing pH on the amount of metal ion adsorbed by the PVA–nano-clay adsorbent could easily be compromised by increasing precipitation of the MOH^+

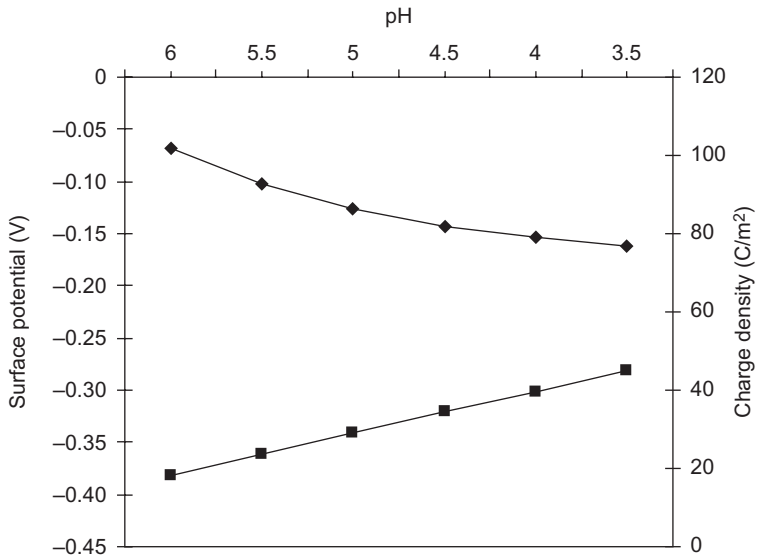

Figure 7. Plots of pH value versus the surface potential (◆) and the charge density (■) of the adsorbent surface. Data obtained from model results using Visual MINTEQA2 version 4.0 software employing a metal ion concentration of 100 mg/ℓ.

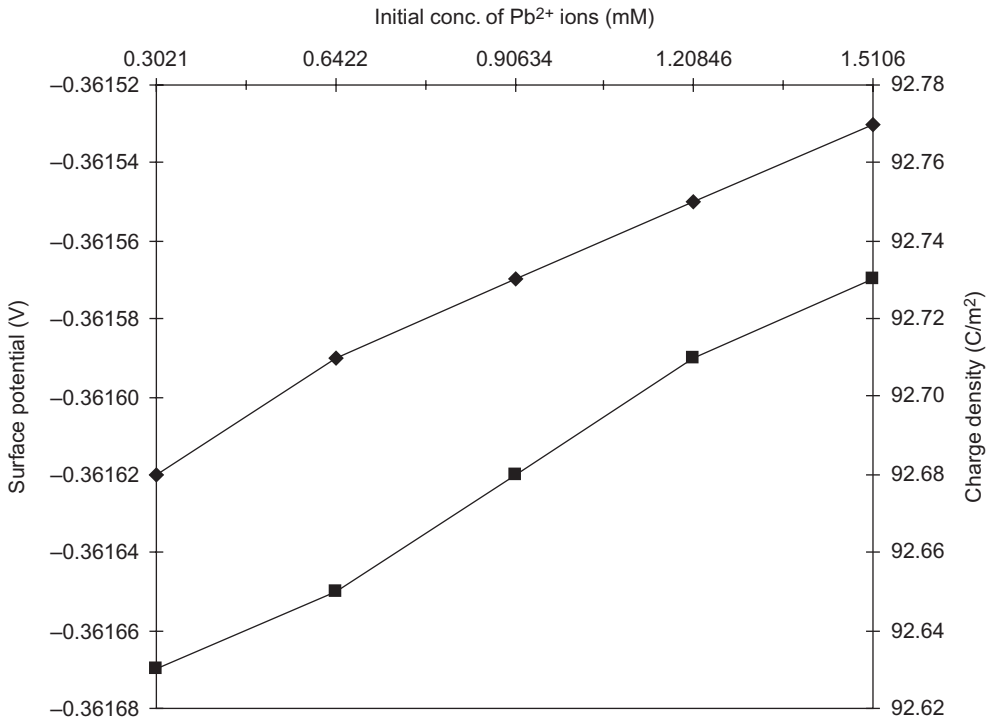

Figure 8. Plots of the initial concentration of Pb^{2+} ions versus the surface potential (◆) and charge density (■) of the adsorbent surface. Data obtained from model results using Visual MINTEQA2 version 4.0 software employing a solution at a pH value of 5.5.

species of both metal ions under these circumstances. Thus, at a pH value of 5.0, 0.073% of the species in the Pb^{2+} ion solution existed as $PbOH^+$, whereas at a pH value of 6.50, 0.010% of the species in the Cd^{2+} ion solution existed as $CdOH^+$ (results from Visual MINTEQA2 version 4.0 modelling at an initial concentration of 500 mg/ℓ for both metal ions, corresponding to 1.5106 mM Pb^{2+} or 4.4480 mM Cd^{2+} ion concentrations, respectively). For this reason, the experiments in this study were undertaken at a pH value of 5.5 to minimize the amount of metal ion precipitated during the adsorption process. Modelling of the adsorption data obtained for an initial concentration of 60 mg/ℓ for both metal ions (see Figure 11), employing our assumed surface site on the PVA–nano-clay, suggests a largely robust fit of the experimental data by the theoretical data produced using the Diffuse Layer Model (DLM) of the surface complexation mechanism in Visual MINTEQA2 version 4.0 software.

From the foregoing, it is plausible to propose that the adsorption of Pb^{2+} and Cd^{2+} ions onto the PVA–nano-clay adsorbent occurred via an inner-sphere surface complexation mechanism as supported by the Diffuse Layer Model for ion adsorption. However, for the unmodified kaolinite clay adsorbent, it has been suggested that the adsorption of Pb^{2+} ions occurs through the formation of unidentate inner-sphere complexes while the adsorption of Cd^{2+} ions occurs onto variably charged sites on the surface of kaolinite through the formation of bidentate complexes (Srivastava *et al*. 2005).

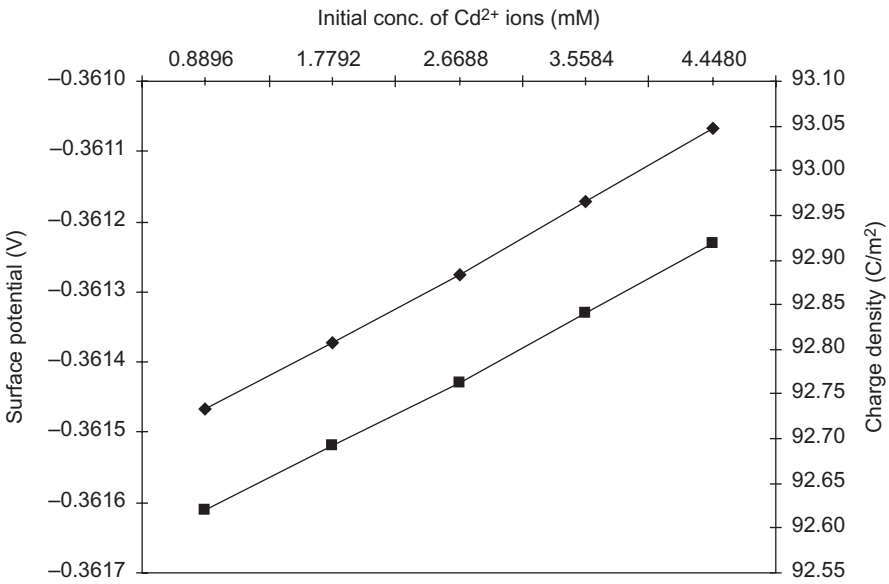

Figure 9. Plots of the initial concentration of Cd^{2+} ions versus the surface potential (◆) and charge density (■) of the adsorbent surface. Data obtained from model results using Visual MINTEQA2 version 4.0 software employing a solution at a pH value of 5.5.

3.6. Equilibrium studies

Table 4 lists the data obtained from equilibrium studies of the PVA–nano-clay adsorbent using the Langmuir isotherm model. It should be noted that the adsorbent showed a stronger preference for Pb^{2+} ions rather than Cd^{2+} ions. Our previous study showed that the adsorption capacities for Pb^{2+} and Cd^{2+} ions onto unmodified kaolinite clay adsorbent were 16.16 mg/g and 10.75 mg/g, respectively (Adebowale *et al*. 2006). In contrast, the PVA–nano-clay adsorbent exhibited an adsorption capacity of 56.18 mg/g and 41.67 mg/g towards Pb^{2+} and Cd^{2+} ions, respectively (see data listed in Table 5). This implies that the adsorption capacity of the PVA–nano-clay was more than three-times greater than that of the unmodified kaolinite clay towards the same ions. This could have arisen because the atomic weight of lead is greater than that of cadmium. In addition, the higher adsorption of Pb^{2+} ions relative to that of Cd^{2+} ions could be ascribed to these adsorbents acting as hard bases which invariably show stronger preferences for borderline metals such as lead rather than for soft acids such as cadmium (Pearson 1963).

3.7. Effect of ionic strength

Varying concentrations of some electrolytes could be present in addition to heavy metal ions in some wastewaters. For this reason, the effect of the presence of typical electrolytes on the adsorption of Pb^{2+} and Cd^{2+} ions onto the PVA–nano-clay was considered to see whether their presence influenced the efficiency of the adsorbent. The data listed in Table 4 show that the simultaneous presence of electrolytes with both Pb^{2+} and Cd^{2+} ions in aqueous solutions reduced the equilibrium adsorption capacity of the PVA–nano-clay adsorbent towards both metal ions.

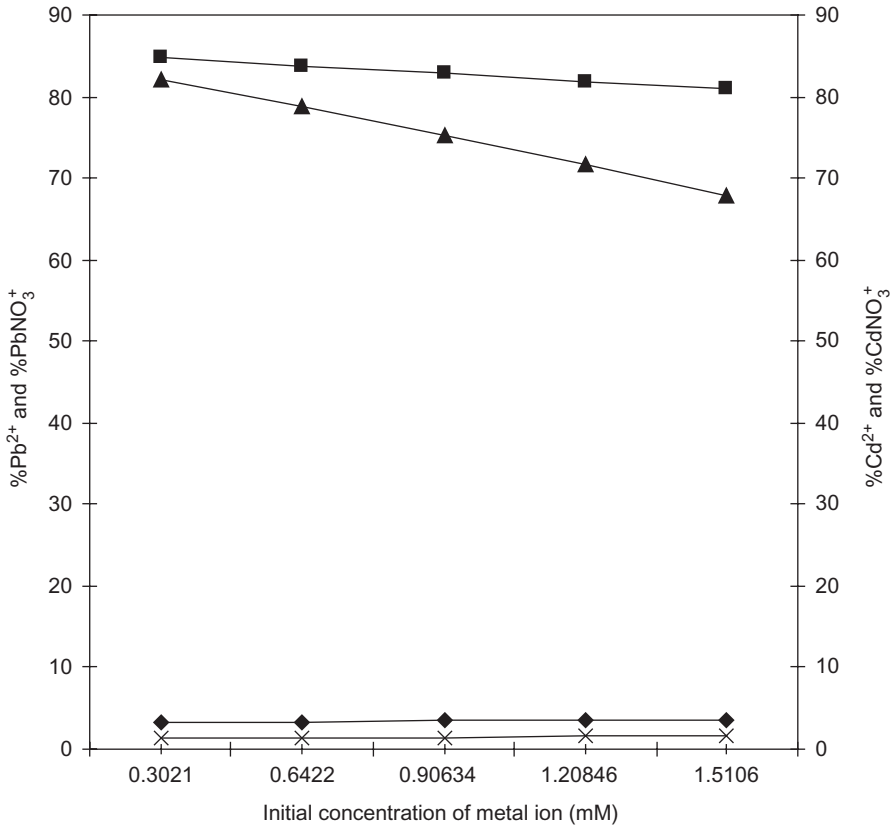

Figure 10. Plots of the initial concentration of metal ions versus the percentage of (■) Pb^{2+}, (◆) $PbNO_3^+$, (▲) Cd^{2+} or (×) $CdNO_3^+$ ions adsorbed onto the PVA–nano-clay surface. Data obtained from model results using Visual MINTEQA2 version 4.0 software for the metal ion solution at a pH value of 5.5.

Thus, in the presence of Na^+ ion-containing electrolytes, a respective decrease of 2.70–15.65% and of 0.43–25.58% was observed for the adsorption of Pb^{2+} and Cd^{2+} ions, respectively, onto the PVA–nano-clay adsorbent. However, with the unmodified kaolinite adsorbent, the corresponding decrease was in the range 0.19–18.38% for Pb^{2+} ions and in the range 33.72–52.76% for Cd^{2+} ions (Adebowale *et al*. 2006).

In contrast, Ca^{2+} ion-containing electrolytes caused a decrease in the adsorption capacity of the PVA–nano-clay adsorbent in the range 17.60–35.28% for the adsorption of Pb^{2+} ions and in the range 2.04–20.01% for the adsorption of Cd^{2+} ions. With the unmodified kaolinite adsorbent, the presence of Ca^{2+} ion-containing electrolytes led to a decrease in adsorption capacity in the range 19.74–48.27% for the adsorption of Pb^{2+} ions and in the range 9.95–37.86% for the adsorption of Cd^{2+} ions (Adebowale *et al*. (2006). Similar trends have been observed by Naidu *et al*. (1994) for the adsorption of Cd^{2+} ions onto soils and by Sparks *et al*. (1995) for the adsorption of Cu^{2+}, Zn^{2+}, Co^{2+} and Cd^{2+} ions onto kaolinite.

This effect of ionic strength on metal ion adsorption is often attributed to the effect of changes in the pH value of the adsorbent/adsorbate suspension on the diffuse double layer (DDL). Thus, it is believed that the presence of electrolytes affects the electrostatic adsorption plane of heavy

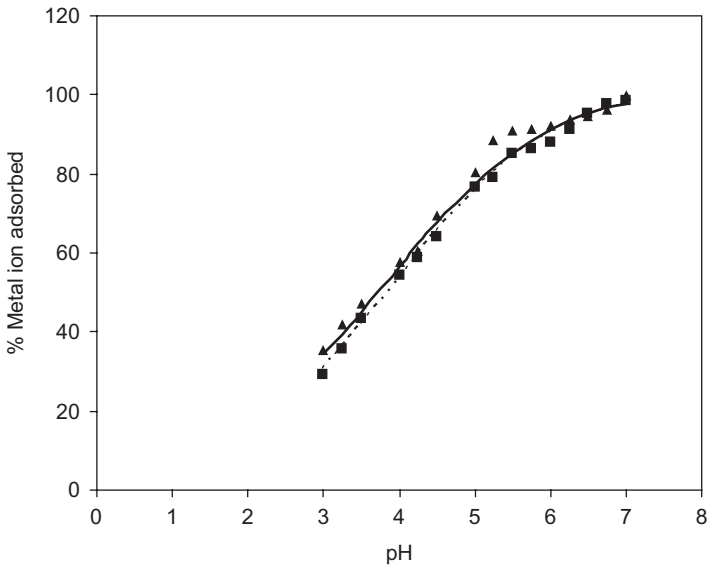

Figure 11. Plots of pH value versus the percentage adsorption of Pb^{2+} or Cd^{2+} ions onto PVA–nano-clay as modelled with Visual MINTEQA2 version 4.0 software. The data points and lines in the figure have the following meanings: ▲, experimental data for Pb^{2+} ions; ■, experimental data for Cd^{2+} ions; ———, model fit for Pb^{2+} ion data; ·····, model fit for Cd^{2+} ion data.

metal ions rather than the surface charge on the adsorbent (Naidu *et al*. 1994). Increasing the ionic strength of the system makes the potential on the adsorbent's surface less negative. Consequently, this has a negative impact on the adsorption capacity of the adsorbent.

The potential in the adsorption plane is related to the valency of the electrolyte cation through its effect on the surface charge density. Increasing the valency of the electrolyte cation decreases the negativity of the potential in the adsorption plane, thereby reducing the extent of metal ion adsorption. Thus, it has been observed that the adsorption of Cd^{2+}, Zn^{2+} and Cu^{2+} ions from aqueous solution decreased as the charge on the cation of the supporting electrolyte increased (Sparks 1989). This explains why Ca^{2+} ion-containing electrolytes have a greater negative impact on the equilibrium adsorption capacity of both PVA–nano-clay and the unmodified kaolinite adsorbent than Na^{+} ion-containing electrolytes.

As far as the effect of anions is concerned, it would appear that the presence of nitrate-containing electrolytes in the system appears to lead to slightly better adsorption of metal ions onto the PVA–nano-clay adsorbent than the presence of chloride-containing electrolytes. This effect was also observed in our previous study with orthophosphate-modified and unmodified kaolinite clay (Adebowale *et al*. 2006). This could be in accord with the assumption of Neal and Sposito (1986) that univalent chloride ions of metallic salts may only be slightly adsorbed.

3.8. Thermodynamic studies

The thermodynamic parameters for the adsorption of Pb^{2+} and Cd^{2+} ions onto the unmodified kaolinite and the PVA–nano-clay adsorbent are listed in Table 5. It will be noted from the data listed that the adsorption of both metal ions onto the PVA–nano-clay adsorbent was exothermic in nature ($\Delta H^0_{mean} < 30$ kJ/mol). This value for ΔH^0_{mean} falls within the range expected for diffusion-controlled adsorption processes (8–22 kJ/mol) as reported by Glasstone *et al*. (1941), thereby

TABLE 4. Effect of Electrolyte on Metal Ion Adsorption onto the PVA–nano-clay Adsorbent.

Parameters[a]	$NaNO_3$			NaCl			$Ca(NO_3)_2$			$CaCl_2$			None[b]
	0.1 M	0.01 M	0.001 M	0.1 M	0.01 M	0.001 M	0.1 M	0.01 M	0.001 M	0.1 M	0.01 M	0.001 M	
Pb^{2+}ions													
Q^0 (mg/g)	47.39	49.02	51.02	47.62	53.76	54.64	36.36	42.55	46.29	37.45	42.92	45.25	56.18
b (ℓ/g)	0.0028	0.0040	0.0064	0.0059	0.0059	0.0069	0.0036	0.0034	0.0050	0.0059	0.0056	0.0053	0.016
R^2	0.9904	0.9944	0.9574	0.8542	0.9130	0.9848	0.9118	0.9354	0.9159	0.8453	0.8824	0.8763	0.9227
Cd^{2+} ions													
Q^0 (mg/g)	35.97	40.32	41.49	35.09	39.84	41.32	33.33	36.76	40.32	36.36	37.88	40.82	41.67
b (ℓ/g)	0.0039	0.0040	0.0044	0.0052	0.0048	0.0052	0.0043	0.0041	0.0040	0.0044	0.0046	0.0043	0.021
R^2	0.9666	0.9568	0.9015	0.9097	0.9354	0.9578	0.9029	0.9356	0.9214	0.9217	0.9154	0.9328	0.9862

[a]Q^0 = maximum adsorption capacity; b = binding energy constant; R^2 = correlation coefficient. [b]None = without electrolyte.

TABLE 5. Thermodynamic Parameters Obtained for the PVA–nano-clay Adsorbent

Pb^{2+} ions				Cd^{2+} ions			
ΔH^0_{mean} (kJ/mol)	ΔS^0_{mean} [J/(mol K)]	ΔG^0 (kJ/mol)	R^2	ΔH^0_{mean} (kJ/mol)	ΔS^0_{mean} [J/(mol K)]	ΔG^0 (kJ/mol)	R^2
–12.48	–76.34	+10.23 at 298 K +11.51 at 313 K +12.11 at 323 K	0.9723	–13.49	–79.93	+10.23 at 298 K +11.51 at 313 K +12.11 at 323 K	0.9534

suggesting that the adsorption of Pb^{2+} and Cd^{2+} ions onto the PVA–nano-clay adsorbent could be largely controlled by diffusion. However, the value of ΔH^0_{mean} since for the adsorption of both ions onto the unmodified kaolinite adsorbent was endothermic (Unuabonah *et al*. 2007).

It should be noted that the calculated ΔH^0 values include the enthalpies of hydration, dilution, mixing and exchange. Uncertainties exist about the energy of hydration of adsorbed/desorbed ions since such terms cannot be calculated with a high degree of accuracy (Udo 1978; Doula *et al*. 1995). Consequently, the ΔH^0 values obtained in the present work are only approximate and can only be employed for qualitative discussions.

The adsorptions of Pb^{2+} and Cd^{2+} ions onto the PVA–nano-clay adsorbent exhibited negative entropies. Such values are to be expected for ΔS^0_{mean} since the internal degrees of freedom of the system decrease during physical adsorption. The ΔS^0_{mean} data for the adsorption of both metal ions onto both adsorbents are listed in Table 5. Gupta *et al*. (2004) have reported negative values of ΔS^0_{mean} for the adsorption of Cd^{2+} and Pb^{2+} ions by Duolite C-433 synthetic resin. The negative value for the entropy change indicates that the metal ion adopted a stable configuration on the adsorbent surface (Gupta and Bhattacharyya 2006) and that no significant changes occurred in the internal structure of the adsorbents (Ozcan and Ozcan 2004).

It will be seen from the data listed in Table 5 that the value of $\Delta S^0_{mean}$for the adsorption of Pb^{2+} ions was higher than that for the adsorption of Cd^{2+} ions. This could suggest that the Pb^{2+} ion forms a more stable complex with both adsorbents while the Cd^{2+} ion only does so with the PVA–nano-clay adsorbent. In part, this might explain the better selectivity shown by the PVA–nano-clay adsorbent towards the Pb^{2+} ion.

The values of ΔG^0 obtained from thermodynamic analysis were found to be small and positive (Table 5), with increasing temperature having little effect on these values. This indicates the presence of an energy barrier in the adsorption process. It has been suggested that a positive value for ΔG^0 is quite common when an ion-exchange mechanism applies in the adsorption of metal ions, because the activated complex formed by the metal ion with the adsorbent is in an excited state (Ozcan and Ozcan 2004).

3.9. Data-fitting analysis

In order to evaluate the fit of an equation to the experimental data from adsorption studies, an estimation of the error involved in the optimization process employed is required. In the present study, the non-linear χ^2-test (Ho and Ofomaja 2005) was used to calculate this error. The χ^2-test statistic is basically the sum of the square of the difference between the experimental data and the data calculated

TABLE 6. Error Analysis for the Tested Adsorption Isotherm Models Using the Non-linear χ^2-Test

Sample	Langmuir model	Freundlich model	Langmuir–Freundlich model	Toth model	Henderson model
Pb^{2+} ions onto					
Unmodified kaolinite	7.93[a]	1.79[a]	13.65[a]	11.72[a]	3.43
PVA–nano-clay adsorbent	2.48	3.80	13.73	17.72	3.88
Cd^{2+} ions onto					
Unmodified kaolinite	8.76[a]	2.04[a]	9.40[a]	17.26[a]	2.75
PVA–nano-clay adsorbent	0.17	0.35	5.49	9.90	0.27

[a]Data reproduced from Adebowale *et al*. (2006).

from the models employed, with each squared difference divided by the corresponding data obtained by calculation from the model. The equivalent mathematical statement is:

$$\chi^2 = \sum \frac{\left(q_e - q_{e,m}\right)^2}{q_{e,m}} \tag{19}$$

where $q_{e,m}$ is the equilibrium capacity (mg/g) obtained from the model by calculation and q_e is the experimental value (mg/g) of the equilibrium capacity. If the data from the model are similar to the experimental data, χ^2 will be small; if they differ, χ^2 will exhibit a larger value.

The non-linear isotherm equations used for this data-fitting analysis are listed in equations (1)–(8) above, while the results of applying the non-linear χ^2-test on the application of these adsorption isotherms to the experimental data are listed in Table 6. It will seen from this table that the Freundlich model gave the best fit for the data for the adsorption of Pb^{2+} and Cd^{2+} ions onto the unmodified kaolinite clay adsorbent, with the lowest χ^2 being 1.79 and 2.04, respectively (Adebowale *et al*. 2006). All the other isotherms tests exhibited higher χ^2 values. The data obtained for the PVA–nano-clay adsorbent showed a better fit to the Langmuir isotherm for the adsorption of both Pb^{2+} and Cd^{2+} ions with χ^2 values of 2.48 and 0.17, respectively. This could suggest that the adsorption sites present on the surface of the unmodified kaolinite clay adsorbent are distributed heterogeneously, whereas those on the PVA–nano-clay adsorbent are homogeneous in nature. The Henderson model also showed good χ^2 values for the adsorption of both metal ions onto the PVA–nano-clay and unmodified kaolinite clay adsorbents, thereby suggesting that more than one mechanism may actually be involved in the adsorption of the metal ions onto the adsorbents studied.

3.10. Desorption kinetics

The desorption of the both metal ions from the unmodified and PVA–nano-clay adsorbents was studied by treating the latter with a 0.1 M aqueous HCl solution. When an initial concentration of 60 mg/ℓ was employed for both metal ions, 99% desorption of these ions was achieved within 3 min of such treatment for both adsorbents. However, when the regenerated adsorbents were subsequently used for the re-adsorption of the metal ions concerned, only 80–90% adsorption was effected for both metal ions. This might have arisen because the acid employed for desorption may have affected the sites available for the adsorption of these metal ions.

4. CONCLUSIONS

Modification of kaolinite clay mineral with polyvinyl alcohol (PVA) increased its adsorption capacity almost three-fold. FT-IR analysis showed that the surface of the resulting PVA–nano-clay adsorbent was occupied by –OH functional groups. The PVA–nano-clay adsorbent was water-stable and could be recycled for re-use within a reasonable period of time (ca. 5 min). The stability of the PVA–nano-clay towards water would allow its ready recovery from filters when employed under industrial circumstances. The adsorption mechanism for Pb^{2+} and Cd^{2+} ions onto the PVA–nano-clay adsorbent was found to be consistent with an inner-sphere surface complexation mechanism involving the diffuse layer model (DLM).

The PVA–nano-clay showed a good adsorption capacity towards both metal ions studied, even in the presence of varying concentrations of electrolytes. The adsorption of Pb^{2+} and Cd^{2+} ions onto the PVA–nano-clay adsorbent was exothermic in nature. This adsorbent shows very good promise as a cheap but efficient adsorbent for the adsorption of Pb^{2+} and Cd^{2+} ions from aqueous solutions. Data-fitting analysis of the adsorption data obtained suggests that the adsorption sites on the PVA–nano-clay adsorbent are homogeneous in nature.

Although the single cycle of adsorption/desorption equilibrium studies undertaken is not sufficient to provide an accurate assessment of the desorption capacity of a given adsorbent, nevertheless this present study has shown that PVA–nano-clay can be regenerated for use in the recovery of Pb^{2+} and Cd^{2+} ions from wastewater streams. The results of the present investigation could be quite useful for further research, especially those directed towards the optimization of the working conditions for the PVA–nano-clay adsorbent. Such studies could certainly be beneficial to both small and medium-sized industries.

ACKNOWLEDGEMENTS

We thank the Chinese Academy of Sciences, CAS, and the Academy of Sciences for the Third World, TWAS, for financial support in the form of a fellowship to E.I. Unuabonah. We especially wish to thank Professor Gangya Zhang of the Institute of Soil Science, Nanjing, P. R. China for the SEM analyses reported. We also acknowledge the support of the Institute of Soil Science, Chinese Academy of Sciences, Nanjing, P. R. China in providing research facilities for this study.

REFERENCES

Adebowale, K.O., Unuabonah, E.I. and Olu-Owolabi, B.I. (2006) *J. Hazard. Mater. B* **134,** 130.
Basar, C.A. (2006) *J. Hazard. Mater. B* **135,** 232.
Bordas, F. and Bourg, A. (2001) *Water, Air, Soil Pollut.* **128,** 391.
Chapman, H.D. (1965) "Cation Exchange Capacity", in *Methods of Soil Analysis, Agronomy*, Black, C.A., Ed, Part 2, pp. 891–901, American Institute of Agronomy, Madison, WI, U.S.A.
Coston, J.A., Fuller, C.C. and Davis, J.A. (1995) *Geochim. Cosmochim. Acta* **59,** 3535.
Dais Filho, N.L., Polito, W.L. and Gushikem, Y. (1995) *Talanta* **42,** 1031.
Doula, M., Ioannou, A. and Dimirkou, A. (1995) *Commun. Soil Sci. Plant Anal.* **26,** 1535.
Frost, R.L., Tran, T.H.T. and Kristof, J. (1997) *Clay Miner.* **32,** 587.
Frost, R.L., Lack, D.A., Paroz, G.N. and Tran, T.H.T. (1999) *Clays Clay Miner.* **47,** 297.
Frost, R.L., Van Der Gaast, S.J., Marek, Z., Kloprogge, J.T. and Paroz, G.N. (2002) *Appl. Clay Sci.* **20,** 177.
Galan, E., Aparicio, P., Miras, A., Michailidis, K. and Tsirambides, A. (1996) *Appl. Clay Sci.* **10,** 477.

Glasstone, S., Laidler, K.J. and Eyring, H. (Eds) (1941) *The Theory of Rate Processes*, McGraw-Hill, New York.
Goldberg, S. (1995) in *Chemical Equilibrium and Reaction Models*, Leoppert, R.H., Schwab, A.P., Goldberg, S., Eds, Special Publication, Vol. 42, Soil Science of America, New York.
Gupta, S.S. and Bhattacharyya, K.G. (2006) *J. Colloid Interface Sci.* **295,** 21.
Gupta, V.K., Singh, P. and Rahman, N. (2004) *J. Colloid Interface Sci.* **275,** 398.
Gustafsson, J.P. (2004) *Visual MINTEQA2 version 4.0: A Computer Program for Speciation*, Department of Land and Water Resources Engineering, KTH, Stockholm, Sweden.
Ho, Y.S. and McKay, G. (1999) *Trans. Chem. E, Part B* **77,** 165.
Ho, Y.S. and Ofomaja, A.E. (2005) *Process Biochem.* **40,** 3455.
Hohl, H. and Stumm, W. (1976) *J. Colloid Interface Sci.* **55,** 281.
Ikhsan, J., Johnson, B.B. and Wells, J.D. (1999) *J. Colloid Interface Sci.* **217,** 403.
Jal, P.K., Patel, S. and Mishra, B.K. (2004) *Talanta* **62,** 1005.
Kinniburgh, D.G., Jackson, M.L. and Syers, J.K. (1976) *Soil Sci. Soc. Am., J.* **40,** 796.
Langmuir, D. (1997) *Aqueous Environmental Geochemistry*, Prentice-Hall, NJ, U.S.A.
Manohar, D.M., Anoop Krishan, K. and Anirudan, T.S. (2002) *Water Res.* **36,** 1609.
Moore, D.M. and Reynolds, Jr., R.C. (1989) *X-Ray Diffraction and the Identification and Analysis of Clay Minerals*, Oxford University Press, Oxford, U.K., pp. 179–201.
Naidu, R.N., Bolan, S., Kookana, R.S. and Tiller, K.G. (1994) *Eur. J. Soil Sci.* **45,** 419.
Neal, R.H. and Sposito, G. (1986) *Soil Sci.* **142,** 164.
Orhan, A.H., Onder, O. and Timur, D. (1998) *J. Colloid Interface Sci.* **198,** 130.
Orumwense, F.F.O. (1996) *J. Chem. Technol. Biotechnol.* **65,** 363.
Ozcan, A.S. and Ozcan, A. (2004) *J. Colloid Interface Sci.* **276,** 39.
Pearson, R.G. (1963) *Soil Sci. Soc. Am., J.* **85,** 3533.
Sang-Mo, K. and Dixon, J.B. (2002) *Appl. Clay Sci.* **18,** 111.
Sears, G.W. (1956) *Anal. Chem.* **28,** 1981.
Shukla, A., Zhang, Y.H., Dubey, P., Margrave, J.L. and Shukla, S.S. (2002) *J. Hazard. Mater.* **95,** 132.
Sidheswara, O., Bhat, A.N. and Ganguli, P. (1990) *Clays Clay Miner.* **38,** 29.
Singh, S.P., Ma, L.Q. and Harris, G.W. (2001) *J. Environ. Qual.* **30,** 1961.
Sparks, D.L. (1989) *Kinetics of Soil Chemical Processes*, Academic Press Inc., New York.
Sparks, K.M., Wells, J.D. and Johnson, B.B. (1995) *Eur. J. Soil Sci.* **46,** 633.
Sposito, G. (1989) *The Chemistry of Soils*, Oxford University Press, New York.
Srivastava, P., Singh, B. and Angove, M. (2005) *J. Colloid Interface Sci.* **290,** 28.
Suraj, G., Iyer, C.S.P. and Lalithambika, M. (1998) *Appl. Clay Sci.* **13,** 293.
Udo, E.J. (1978) *Soil Sci. Soc. Am., J.* **42,** 556.
Unuabonah, E.I., Adebowale, K.O. and Olu-Owolabi, B.I. (2007) *J. Hazard. Mater.* **144,** 386.
Unuabonah, E.I., Olu-Owolabi, B.I., Adebowale, K.O. and Ofomaja, A.E. (2007) *Colloids Surf. A* **292,** 202.